

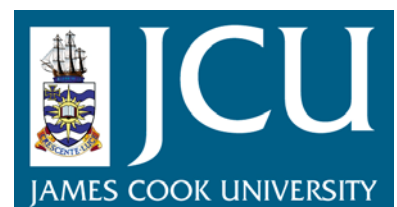
JCU ePrints

This file is part of the following reference:

Henderson, David James (2010) *Response of pierced fixed metal roof cladding to fluctuating wind loads.* PhD thesis, James Cook University.

Access to this file is available from:

<http://eprints.jcu.edu.au/12173>



James Cook University

SCHOOL OF ENGINEERING AND PHYSICAL SCIENCES

**Response of pierced fixed metal roof cladding to
fluctuating wind loads**

Thesis submitted by

David James Henderson BEng(Hons)

in April 2010

for the degree of Doctor of Philosophy

in the School of Engineering and Physical Sciences

James Cook University

In memory of my father,

R. D. Henderson

17 Sept 1939 – 4 Nov 2008

Statement of access

I, the undersigned, the author of this thesis, understand that James Cook University will make it available for use within the University Library and via the Australian Digital Theses network for use elsewhere.

I understand that as an unpublished work a thesis has significant protection under the Copyright act and I do not wish to place restrictions on access to this work.

.....
David Henderson

.....
Date

Statement of sources

I declare that this thesis is my work and has not been submitted for another degree or diploma at any university or other institution of tertiary education. Information derived from published or unpublished work of others has been acknowledged in the text and a list of references is given.

.....

David Henderson

.....

Date

Statement on the contribution of others

This thesis included the following contributions of others:

Grants: This work was supported by an ARC Linkage grant with a major funding contribution from Stramit Corporation Pty Limited as the industry partner. Additional funding was received from the School of Engineering and Physical Sciences at James Cook University (JCU) through the Uninet grant. A travel stipend was awarded by the Australasian Wind Engineering Society to present a paper at an international conference. The Cyclone Testing Station (CTS) provided funds to assist in the transportation of the Pressure Loading Actuator (PLA).

Supervision: A/Prof J. D. Ginger (JCU) was the principal supervisor of this work. Other supervision was from A/Prof G. A. Kopp (UWO). In the early stages of the project Prof C. C. Berndt (Swin) and A/Prof W. Karunasena (USQ) were also supervisors.

Editorial Assistance: Principal editorial assistance was provided by A/Prof J. D. Ginger at JCU and A/Prof G. A. Kopp at the University of Western Ontario (UWO). Additional assistance was provided by my Mum, A/Prof L. D. Henderson at JCU who is still arguing about the word, 'roofs'.

Experimental infrastructure: Bluescope Steel provided assistance in conducting some of the tensile test specimens. Mr C. Arrowsmith provided assistance in the fabrication of the air-chamber. Mr W. Morris provided assistance in the fabrication of the camera slide. Labview PLA control software, coded by Mr M. Morrison, was modified for use in this work. A rainflow analysis coded by Prof Y. L. Xu, was modified for this work. UWO provided a prototype PLA that enabled the major component of the experimental work to be undertaken. Wind tunnel model time series data was obtained from the NIST data base and from UWO.

Acknowledgements

I first and foremost thank A/Prof John Ginger for his guidance, support and all his patience throughout this work. I also thank A/Prof Greg Kopp for his advice and guidance.

I acknowledge the support of an Australian Research Council Linkage Grant and Stramit Building Products as the industry partner. I would like to thank Dr Subo Gowripalan and Mr Chris Healy from Stramit for their support and discussions about this project.

I would like to thank Prof Mahen Mahendran for early discussions on this project as well as Prof Chris Berndt and Prof Karu Karunasena.

Thanks also go to A/Prof Greg Kopp, A/Prof Mike Bartlett and Prof Dave Surry from the University of Western Ontario, for providing a Pressure Loading Actuator to advance the Station's research into wind induced fatigue of cladding.

I would like to very much thank my friends and colleagues from the Cyclone Testing Station and JCU, both past and present: Mr Greg Reardon, Mr Cam Leitch, Mr Wayne Morris, Mr Graeme Stark, Mr Don Braddick, Mr Curt Arrowsmith, Dr Barbara Kennedy and Prof John Patterson, for their support and advice.

Many thanks are due to fellow post-grad students at UWO: Mr Murray Morrison and Dr Eri Gavanski, and to Ms Yadan Mao at JCU, for their fruitful discussions and encouragement.

And, as it is traditional, necessary and accurate, I would like to thank my family: Anne, Dawn, Lyn, Mike, Barbara and Don for their patience and support.

Abstract

The roof of a low rise building (e.g., house, industrial shed) is subjected to intense fluctuating wind pressures during a tropical cyclone. A failure of the building's roof is not only a life safety issue but also impacts greatly on the community's resilience during and after wind storms.

Low cycle fatigue cracking of roof and wall cladding, fixings, and supports during tropical cyclones is a complex process, where small changes in load, geometry or material properties can significantly affect the fatigue performance of the cladding system. Investigating the performance of the building envelope when subjected to cyclonic winds is of importance to the manufacturing and construction industry, and standards communities. A better understanding of the fatigue mechanisms of cladding systems will provide industry with a means to optimise the cladding design and to improve the assessment of vulnerability of building stock.

The research was conducted to analyse the performance of light gauge but high yield strength corrugated metal cladding subjected to cyclonic wind loads. The experimental methods involved tensile coupon tests and static point load tests as well as static pressure, cyclic pressure and dynamic wind pressure tests on double 900 mm span 0.42 mm BMT G550 corrugated cladding specimens. The air pressure tests, including the simulated cyclonic wind pressures, were carried out by using a Pressure Loading Actuator (PLA) that was able to apply a positive and negative (suction) pressure via an air-chamber. Reactions in the X, Y and Z directions were measured at the cladding screws, along with lateral movement of the screws and crack growth in the cladding under the range of fluctuating loads.

Wind tunnel test data and full scale measurements show that the wind pressures are highly fluctuating and temporally and spatially varying across the building envelope. Yet the line load testing and typical product testing applies the "same load" to all fasteners in the test specimen. The thesis has shown, by measuring fastener reactions to point loads applied at various points across the cladding, that there is minimal influence on the reaction in one screwed crest to an adjacent screwed crest, justifying the assumption of applying a uniform load across the test specimen.

Different shaped cyclic pressure traces, such as sinusoidal, sawtooth and spike were used. The numbers of cycles to failure for these pressure traces with similar load cycle ranges showed it was the peak load per cycle and load ratio that governed number of cycles to failure and not the RMS of the trace or the duration of the peak.

The application of fluctuating pressures representing wind loads enabled the assessment of cladding response to these dynamic pressures and a comparison to cyclic load tests. Cladding crack patterns generated with the simulated wind trace from the PLA were similar in shape and length to crack patterns reported in damage surveys and the loads at which the claddings deformed and buckled, were of similar magnitude to those in the cyclic load tests. Analysis of the applied fluctuating pressures and resultant screw reactions showed that the cladding specimens responded in a quasi-static manner. That is, there was no resonance in the cladding from the fluctuating pressures.

A Damage Index metric based on S_{\max} -N cyclic test data is proposed that could be used as an indicator of extensive cladding damage and possible cladding failure for generated cyclonic traces. The DI could also be used to indicate possible crack initiation for crease type cracks following low intensity cyclone crossings.

The outcomes of this study have demonstrated (a) the relevance of the experimental basis of the current test standard (i.e., L-H-L), (b) the improved resilience of the building envelope if designed to the L-H-L standard over the previous test criteria, (c) potential areas to be strengthened in current building stock, and (d) the need for increased design pressures on cladding elements in the Australian Wind Actions Standard.

Table of Contents

1.	Introduction	15
1.1	Objectives	17
1.2	Overview	17
2.	Literature review	19
2.1	Northern Australian metal roofing	19
2.1.1	Roof envelope	19
2.1.2	Light gauge metal roofing	20
2.1.3	G550 properties	21
2.2	Fatigue failure	22
2.2.1	Failure modes	22
2.2.2	Load cycles	23
2.2.3	Miner’s rule	23
2.2.4	Fracture mechanics	24
2.2.5	Variable amplitude loading	27
2.2.6	Fracture mechanics design strategies	27
2.2.7	Short fatigue cracks	27
2.3	Fracture toughness of G550 flat sheet	28
2.4	Fatigue performance of G550 cladding	28
2.5	Wind loading	32
2.5.1	Tropical Cyclones	32
2.5.2	Wind loading as defined by the Building Code and Australian Standard	34
2.5.3	Wind loads on low rise buildings	36
2.5.4	Load cycles from wind	38
2.5.5	Australian wind fatigue test criteria	41
2.6	Physical testing methods	44
2.6.1	Single fastener pull through	44
2.6.2	Line load testing	45
2.6.3	Air-bag	47
2.6.4	Air-box (free air)	48
2.6.5	Simulated wind load	48
2.7	Numerical methods	51
2.7.1	Modelling of cladding	51
2.7.2	Modelling of cladding with load cycles	52
2.8	Summary	53
3.	Experimental configurations and procedures	54
3.1	Tensile tests	54
3.2	Pressure loading and measuring response of cladding systems	54
3.2.1	Loading system (PLA at JCU)	55
3.2.2	Air-chamber	58
3.2.3	Measurements during testing	63
3.3	Point load tests (influence line test method)	68
3.4	Summary	70
4.	Response of cladding to static and cyclic loading	72
4.1	Static uniform pressure loading	72
4.1.1	Loading in elastic range	73
4.1.2	Loading in plastic range	75
4.1.3	Summary of static loading	80
4.2	Cyclic loading	81
4.2.1	Cycles to failure – Overall results	81
4.2.2	RMS of pressure for different shaped load cycles	82
4.3	Crack patterns	85
4.3.1	Crack initiation	86
4.3.2	‘H’ crack group	86

4.3.3	Star crack type	90
4.4	Variation in load cycles to failure	97
4.4.1	Failures of cladding at screws	99
4.4.2	Different coil strengths	99
4.4.3	Effect of contact area under screw head	100
4.4.4	Screw fixed into Z-purlin	102
4.4.5	Cladding failing at an adjacent screw to load cell	103
4.5	Comparison of air-chamber cyclic loading to line loading	105
4.6	Summary of cyclic loading	106
5.	Wind loading tributary area for a cladding screw	108
5.1	Point load testing (Influence coefficient)	108
5.2	Wind loads acting on a cladding screw tributary area	110
5.3	Summary	116
6.	Response to laboratory simulated cyclonic wind loads	117
6.1	Selection of representative fluctuating wind pressures	117
6.1.1	Building geometry	120
6.2	Wind loads from AS/NZS 1170.2	123
6.3	Wind tunnel data	124
6.4	“Design” cyclonic wind trace	126
6.5	Response of cladding to dynamic wind load	130
6.5.1	Comparison of “design” cyclone wind trace to L-H-L	134
6.5.2	Failure of cladding from simulated wind load	135
6.6	Use of a Damage Index to compare traces	138
6.6.1	Limitations and assumptions of the DI	142
6.6.2	Crack initiation estimate using DI	144
6.7	Variations in peak pressures and load cycle distributions	144
6.7.1	Comparison of Open and Suburban terrain	144
6.7.2	Roof slope and shape	147
6.7.3	Placement of dominant opening	148
6.7.4	Comparison of “design” cyclone to cyclone events	150
6.8	Comparison of pressure traces with L-H-L	153
7.	Conclusions and recommendations	157
7.1	Recommendations for further research	160
7.2	Recommendations for building design	161
7.3	Concluding statement	163
8.	References	164
Appendix A.	Air-chamber trials	169
Appendix B.	Data for area of cladding screw study	182
Appendix C.	Pressure time series data	185
Appendix D.	Generated pressure traces based on actual cyclone events	197

List of Figures

Figure 1.1: (a) Catastrophic failure of metal roof cladding, and (b) Cladding pulling over heads of fasteners (CTS collection)	15
Figure 2.1: Multi-hip roof on recently constructed house	19
Figure 2.2: Roof under construction	19
Figure 2.3: Industrial shed.....	20
Figure 2.4: Common profiles of metal sheet cladding (Stramit 2006).....	21
Figure 2.5: Orientation of tensile test coupons (Rogers and Hancock 1997).....	22
Figure 2.6: Load cycles	23
Figure 2.7: Logarithmic crack growth rate (Smith 1991)	26
Figure 2.8: LPD of corrugated cladding under screw head.....	29
Figure 2.9: Constant amplitude block loading (Mahendran 1989).....	30
Figure 2.10: Crack patterns from constant amplitude cyclic loading (Xu 1995b).....	31
Figure 2.11: S-N curve for corrugated cladding fastened without cyclone washers (Mahendran 1989).....	31
Figure 2.12: Cycles to failure (Henderson and Ginger 2005)	32
Figure 2.13: Wind Regions of Australia (Standards-Australia 2002b)	35
Figure 2.14: Pressure coefficients for a low rise building (Kopp <i>et al.</i> 2010)	36
Figure 2.15: Representation of wind forces on a house from a design standard.....	37
Figure 2.16: Design wind forces with a dominant opening in windward wall.....	37
Figure 2.17: Geometry of Texas Tech full scale test building (Ginger 2001)	39
Figure 2.18: Pressure coefficients for Area A (Ginger 2001)	39
Figure 2.19: Cyclic load regimes (Henderson <i>et al.</i> 2001)	42
Figure 2.20: Line load test rig (Mahendran 1993) for loading of a cladding sample.....	46
Figure 2.21: Failure of cladding at lap during testing at CTS	48
Figure 2.22: MSU metal cladding test rig (Surry <i>et al.</i> 2007).....	49
Figure 2.23: FEA model of rib-pan cladding (Mahaarachchi and Mahendran 2004) (a) detail of mesh at fixing hole (b) model of half width sheet of cladding (c) model of one rib ..	52
Figure 3.1: Pressure loading actuator (PLA).....	56
Figure 3.2: Plot of PLA achieved response against the requested target real time pressure trace ..	57
Figure 3.3: Air-chamber in Configuration A with Z-purlin prior to installation of cladding.....	58
Figure 3.4: Air-chamber in Configuration B mode showing the load cells and screw stubs	59
Figure 3.5: Sketch of cladding with edge strips and screw numbering.....	60
Figure 3.6: Load cells with screw stubs for Configuration B	65
Figure 3.7: X, Y and Z axis for JR3	65
Figure 3.8: Point load test setup.....	68
Figure 3.9: Load cell details for measurement of (a) screw reaction at the first internal support and (b) applied point load at mid-span of the first cladding span	69
Figure 3.10: Sketch showing screw numbering, purlin spacing and loading position grid.....	70
Figure 4.1: Location of screws S1 to S6 and displacement transducers d1 to d5 for Configuration A	73
Figure 4.2: Positions of strain gauges sg1 to sg6 located at screw S3 (strain gauges on top surface)	73
Figure 4.3: Ramped static load step trace to 2 kPa	74
Figure 4.4: Stresses at strain gauge locations for the loading and unloading ramped pressure trace to 2 kPa	74
Figure 4.5: Change in stresses for pressures in steps up to 4 kPa	75
Figure 4.6: Displacement of cladding for stepped pressure trace up to 4 kPa	76
Figure 4.7: Plastic deformation of cladding at top of the crest adjacent to the screw for applied pressure of 4 kPa.....	76
Figure 4.8: Large distortional changes in cladding for stepped pressure trace up to 5 kPa	77

Figure 4.9: Permanent transverse creasing at flattened screwed crests with the screwed corrugations almost inverting and the unscrewed crests deflecting upwards approximately 30 mm at 5 kPa	78
Figure 4.10: Static step loading (pressure-blue, coefficient-red, Z reaction-black).....	79
Figure 4.11: X, Y and Z components of central screw reaction.....	79
Figure 4.12: Applied line load versus fastener reaction (Xu 1992)	80
Figure 4.13: P versus N for cyclic loading with varying R values.....	82
Figure 4.14: Cyclic pressure traces showing the profile shapes used	83
Figure 4.15: RMS of pressure traces versus numbers of cycles to failure	84
Figure 4.16: P_{max} versus N for different trace types with different R ratios	84
Figure 4.17: Example of (a) 'H' type and (b) 'Star' type crack patterns	85
Figure 4.18: Number of cycles to crack initiation and to failure with crack type.....	85
Figure 4.19: Development of H type crack	87
Figure 4.20: Movement of screw over time	88
Figure 4.21: X and Y Displacement of screw from start location.....	89
Figure 4.22: Reactions in X, Y and Z directions at start of test	89
Figure 4.23: Z reaction (uplift) at screw compared to applied pressure.....	90
Figure 4.24: Deformation of crest of cladding under screw head in Configuration A.....	91
Figure 4.25: Cracks in cladding protruding from under screw head.....	91
Figure 4.26: Extension of cracks and deformation of cladding with cladding bearing on flanges of screw	92
Figure 4.27: Star crack failure (note rub marks from screw flanges).....	92
Figure 4.28: Star crack and dishing under screw head in Configuration B (Photo at 1800 cycles)	92
Figure 4.29: Star crack and cladding deformation during a load cycle (Note sloped deformation of seal).....	93
Figure 4.30: Displacement of screw for two time periods	93
Figure 4.31: X, Y and Z reactions at screw over 10 sec periods at initial, mid and final stages of the trial.....	94
Figure 4.32: Reduction in Reaction Coefficient for the peaks of each load cycle for the duration of the trial.....	95
Figure 4.33: Total peak reaction force at central support (Xu 1995b)	96
Figure 4.34: Reaction coefficient variation with pressure and time.....	96
Figure 4.35: Comparison of Coil-A and Coil-B.....	100
Figure 4.36: Cracking of cladding without EPDM seal under screw head	101
Figure 4.37: Cracking of cladding with an EPDM seal under screw head.....	101
Figure 4.38: Movement of screw head when fixing cladding to Z purlin.....	102
Figure 4.39: Rotation of screw head during load cycles	103
Figure 4.40: Applied pressure and uplift load on JR3 at S3.....	104
Figure 4.41: X, Y and Z reactions with Resultant force at S3	104
Figure 4.42: Peak pressure with numbers of cycles to failure from the air-chamber trials and for Xu (1995b) line load test data.....	105
Figure 4.43: Peak load per screw versus number of cycles to failure for line load test rig (Mahendran 1989) and air-chamber (PLA) trials	106
Figure 5.1: Contour of Influence coefficients for uplift reaction at S2	109
Figure 5.2: Influence coefficient along length of cladding crest line containing screw S2	109
Figure 5.3: Reduction in peak pressures for increasing area (Surry <i>et al.</i> 2007)	111
Figure 5.4: Corner region of building showing contours of minimum peak pressure coefficients for 0°, 30° and 45° wind angles.....	112
Figure 5.5: Snapshot of contours of pressure coefficients for 51 taps in the corner region for 0° wind direction, at three different time stamps	114
Figure 5.6: Snapshot of contours of pressure coefficients for wind angles of 30°, 45° and 90° for 51 taps in the corner region	114
Figure 6.1: Wind speed and direction for Cyclone Vance (Reardon <i>et al.</i> 1999)	118
Figure 6.2: Track of Cyclone Vance with location of Larnmonth relative to path of eye (Bureau of Meteorology track map (Reardon <i>et al.</i> 1999))	118

Figure 6.3: Variation of mean wind speed and direction over time (Jancauskas <i>et al.</i> , 1994).....	119
Figure 6.4: Histogram of cladding end span to building eaves height ratio.....	121
Figure 6.5: Diagram of Building 5-5 including location of pressure taps.....	122
Figure 6.6: Peak and mean C_p for Areas A, B and C and Wall W_L for Building 5-5.....	125
Figure 6.7: Peak and mean pressures for Building 5-5 for orientations 25 and 75	127
Figure 6.8: Pressures for varying wind angle and mean wind speed over time for Building 5-5, orientation 25 (dominant opening created at 135 minutes)	129
Figure 6.9: Net pressures for varying wind angle and mean wind speed over time for Building 5-5, orientation 75 (dominant opening at W_L for entire duration)	129
Figure 6.10: Cracking of cladding at screw fixing for Building 5-5, orientation 25.....	131
Figure 6.11: Reaction coefficient (RC) over three time spans of the design cyclone	131
Figure 6.12: Spectrum of equivalent reaction (pressure \times idealised area) and reaction at screw for three time spans of “design” cyclone trace.....	132
Figure 6.13: X, Y and Z reactions measured by JR3 “screw” for “design” cyclone trace for interval 135 to 205 minutes	133
Figure 6.14: (a) Crack pattern of JR3 “screw” showing crease points in the same cladding span with (b) corresponding 3d plot of reactions at “screw”	134
Figure 6.15: Cracking patterns following L-H-L tests of cladding that (a) failed and (b) passed but had a 15% reduction in load per cycle.....	135
Figure 6.16: Applied pressure trace showing failure at -6.6 kPa at 123 minutes.....	136
Figure 6.17: Movement at screw head showing jump at 75 minutes	136
Figure 6.18: Roofing system “failed” by cladding cracking and pulling over head of screw (PLA test W6).....	137
Figure 6.19: Crack patterns from corrugated cladding after Cyclone Tracy (Beck 1975).....	137
Figure 6.20: S_{max-N} for corrugated cladding screw fixed at alternate crests.....	139
Figure 6.21: Building 5-5, orientation 25, in suburban terrain with a dominant opening occurring on long wall at 135 minutes.....	146
Figure 6.22: Pressure trace in open terrain for Building 5-5 orientation 25 with a dominant opening in gable end wall for whole trace.....	149
Figure 6.23: SEA modelled and “design” mean wind speed and Wind direction.....	150
Figure 6.24: Pressure trace for bo1 in Alawa.....	151
Figure 6.25: Mean wind speed and direction from AWS for Exmouth (Learmonth).....	152
Figure 6.26: Number of cycles from rainflow analysis for generated traces	154
Figure 6.27: Comparison of cycle numbers from rainflow analysis with peak pressure for generated traces and L-H-L	155
Figure 6.28: Possible reduction in loads per cycle for L-H-L.....	156

List of Tables

Table 2.1: Australian tropical cyclone category scale.....	33
Table 2.2: Table B1.2a and B1.2b from Building Code of Australia (2007).....	34
Table 2.3: Distribution of net pressure cycles (Henderson and Ginger 2005).....	40
Table 4.1: Variation in load cycles for $R=0.4$	97
Table 4.2: Variations in cycles to failure for line load tests (Mahendran 1989).....	98
Table 4.3: Variation in cycles to failure for $R=0$ with initial load at load cell “screws”.....	98
Table 4.4: Aggregation of crack extents for cyclic loading.....	99
Table 4.5: Comparison of number of cycles to failure for Z-purlin.....	103
Table 5.1: Influence coefficients for the uplift reaction at screw S2.....	108
Table 5.2: Vertical movement of cladding for point loads at locations along crest line S2.....	109
Table 5.3: Comparison of area averaging method with direction.....	113
Table 5.4: Rainflow cycle counts of pressure coefficient for screw 409 for 30° wind angle.....	115
Table 6.1: Data from survey of 26 industrial sheds from Townsville region.....	121
Table 6.2: Design pressures for Building 5-5 using AS/NZS1170.2.....	124
Table 6.3: Numbers of cycles for external and net pressures (kPa) for building 5-5 orientation 25	140
Table 6.4: Numbers of cycles for external and net pressures (kPa) for building 5-5 orientation 75	141
Table 6.5: Simulated wind load tests with DI values.....	142
Table 6.6: Building 5-5 external and net pressures for open and suburban terrain.....	145
Table 6.7: Building 5-14 external and net pressures for open and suburban terrain.....	145
Table 6.8: Percentage of cycles with $R = 0$ within each 10% range column of the rainflow matrix	147